Cyclotron Improvements

P. S. Miller, H. G. Blosser, H. Hilbert, E. Kashy, D. Magistro, P. Marchand and G. Stork

I. Center Plug and Source Mount Operation

The advantages of attaching the ion source, puller and 180° selection slit rigidly to the cyclotron magnet were discussed in the 1971-1972 Annual Report in connection with our plans to install a new 6" diameter center plug through the lower pole tip. This plug has been in use continuously since March 1973. At first only the 180° selection slit was installed on the plug. The old ion source, inserted through the upper pole, was used while new ion sources and associated components were fabricated. In March 1974 the lower plug source for first harmonic operation was tested in the cyclotron. Since May it has been in routine use. The source for second harmonic was finished in June 1974 and also performs satisfactorily.

A suitable design for the insulator to hold the puller is still being sought. Freon-cooled alumina appears to be the most promising type. Our initial design, which was an adaptation of an existing insulator, was tested at dee voltages in excess of 55 kV but usually failed in less than 3 hours by developing leaks, sometimes at the seals and other times as cracks in the insulator. A new insulator was designed with axial cooling symmetry and a base geometry that keeps rf currents away from the gaskets. These insulators are now being manufactured for us.

We have tried insulators made of other materials, namely boron nitride, Corning type 9658 machineable glass ceramic, and quartz (uncooled thin-wall tube), all of which have failed too rapidly to appear promising.

II. DC Extraction Electrode for Ion Source

In a cyclotron with an internal ion source the rf dee potential extracts ions from the plasma of the ion source into the machine. The transit time from the source to the puller is always a substantial fraction of an rf cycle (60 rf degrees in the MSU cyclotron in first harmonic). The large magnitude of the transit time makes the third harmonic mode unusable in our cyclotron and adversely affects the quality of second harmonic beams.

To offset this difficulty we have installed a DC extraction electrode in front of the ion source slit in the manner suggested by Mallory, et al.[1] This electrode is biased to continuously extract ions regardless of the dee potential. The electrode has been used successfully on first harmonic proton beams with a bias of 3 kV. The electrode is a tungten plate placed 1 mm in front of the source and containing a single slit through which the ions pass. Encouraged by the success of this test, we are going ahead with the modifications required for using the grid in second harmonic operation.

III. Magnetic Field Monitors

Four pickup coils, each containing about 5000 turns, have been installed inside one of the dummy dees for monitoring magnetic field fluctuations. Since there are eight trim coils in the MSU cyclotron the monitor coils were placed as nearly as possible at locations between adjacent trim coils. The magnitude of the alternating magnetic field resulting from an alternating current in a trim coil is attenuated rapidly with increasing distance from the coil windings by eddy currents in the copper liner of the rf cavity. Four pickups allow sensitive monitoring of every trim coil and are easier to interpret than one pickup.

The output signals are amplified by four integrating amplifiers whose outputs are calibrated directly in magnetic field units and displayed on an oscilloscope.

IV. Detector Cooling Refrigerators

To cool silicon detectors in the past we have circulated alcohol cooled by dry ice through the detector mounts. Before breaking vacuum in the detector chamber the alcohol was warmed by means of a heat exchanger using hot water as a heat source. Recently several conventional freon refrigeration systems have been set up to take over these functions. The freon refrigerent itself is circulated through the detector mount. To heat the detector, the freon flow is reversed so that it gets hot. The refrigerators are mounted on wheeled hand trucks for portability.

This system is more convenient than the old arrangement and is expected to save several hundred dollars a year in dry ice costs.

V. Dee Voltage Measurements with X-Rays

Calibration of the rf voltmeters used to measure and stabilize the amplitude of the dee voltage is difficult to perform accurately in most cyclotrons. At MSU the individual turns can be resolved by a beam probe. Thus the sum of the amplitudes for the 2 dees can be calculated accurately from a turn count and the known beam energy. The ratio or difference between the voltage on the two dees is more difficult to determine, especially since the response of the voltage pickups is frequency-dependent.

We have found that the endpoint energy of the bremstrahlung radiation which is always produced when the cyclotron is running can be used to measure the dee coltage with an uncertainty of about 1 kV, estimated by analyzing the graphical procedure used to infer the endpoint energy. Figure 1 gives

the result of a first set of measurements. The detector with an energy resolution of 1 keV FWHM measured with the 122 keV radiation from a ^{57}Co source. No corrections need to be made for the electron transit time from dee to ground plane since this time is always less than 5 rf degrees ($\Delta E/E = 0.4\%$).

REFERENCES

1. M. Mallory, E. Hudson and R. Lord, IEEE Trans. on Nuc. Sci. NS-20 #3, 147(1973).

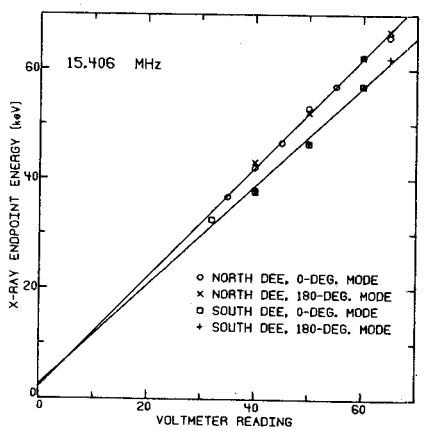

Fig. 1.--Calibration curves for the dee voltmeters in the MSU cyclotron. The data imply no dependence on the rf mode. The straight lines are visual fits to the data.

A Pulse Generator for Slow Beam Pulsing

J.-F. P. Marchand and T. L. Khoo

Introduction

The pulsed beam structure of our cyclotron is ideally suited for measuring isomeric lifetimes of $\lesssim$50 ns. For longer lifetimes it is necessary to lengthen the period between beam pulses and we have used a beam sweeper[1] to obtain pulse periods of $\lesssim$600 ns. For longer-lived isomers, it is necessary to increase the beam-off time and for this purpose a beam pulser has been constructed which allows the beam to be turned on and off according to the requirements of the experiment. An important requirement of such a beam pulser is that it should turn the beam off as quickly as possible, so that the sample to be measured has no time to decay much during the transcient period. A way to intercept the beam is to deflect it with an electric field across a pair of slits (Figure 1). A voltage across two electrodes mounted on both sides of the trajectory of the beam will cause it to be deflected from a straight line. The deflection at the slits (S) is then given by (for particles of unit charge):

$$D_S(V) = \frac{V}{d}\frac{1}{2E}\,\ell\left(\frac{\ell}{2} + L\right) \text{ for } D_S \ll L$$

V = Voltage across electrodes (V)

d = Distance between electrodes (m)

E = Energy of particles (eV)

ℓ = Length of electrodes (m)

L = Distance of travel to slits (m)

The dimensions for our deflection electrodes are

$$d = 2.5^{*}10^{-2}(M)\ell = 1(M), L = 3.4(M)$$

Thus for 50 MeV protons, for example, the deflection is 1.56 mm/kV. The next paragraph describes a beam pulser that will produce pulses of 3-4 kV, with a rise time of 1 μsec and a maximum repetition rate of 25 KHz.

The Beam Pulser

Figure 2 shows a simplified diagram of the beam pulser. Basically the beam pulser consists of two parts, a vacuum tube switch and a pulse generator. The input is a TTL-level logic signal. During the low state of the input signal the vacuum tube will be driven into the conducting state, thus shorting the electrode to ground. In this state the voltage on the electrode will be near zero.

With the positive transcient of the input signal the control logic will trigger the pulse generator. It will then generate a fast rising pulse to charge the deflecting electrode to a voltage of approximately 4 kV. A small 5 kV power supply with an 1 MΩ resistor is provided to insure that the electrode will stay at a high potential until the vacuum-tube is driven into conduction again.

The advantage of this circuit is that power is only dissipated during the positive transients of the deflecting voltage.

Figure 3 shows some wave forms in the pulse generator. In the quiescent state transistor Q_1 is conducting, and there is no current through Q_2 and Q_3 and the primary (P) of the toroidal ferrite core transformer T. The generator is triggered by applying a negative going pulse at the base of Q_1. Transistors Q_2 and Q_3 will then start conducting, current will start flowing through the primary (P), and a voltage is induced in secondary S_1. This voltage is fed back to the bases of Q_2 and Q_3, thus closing a feedback-loop. For one cycle the generator will thus oscillate strongly with primary currents of some 20A. The voltage induced into the secondary will first be negative (~1500V) charging capacitor C through diode D_1. With the positive transcient the deflecting plate will be charged via C and D_2. Diodes D_1 and D_2 and capacitor C thus form a voltage-doubler.

The total delay from triggering to the charging of the electrode is 5 sec; the rise-time of the voltage at the electrode is 1 sec. The maximum repetition-rate for full pulse-height is 25 KHz, this limit being due to power supply limitations (2A@50V). The pulser may be operated periodically or in a on-demand mode.

Figure 4 shows the time-structure of the beam at the target. This was measured by monitoring 48 MeV α particles, scattered from the target, with a Si detector. The turn-off time (90%-10%) of the beam in this case is 1.4 μsec.

Figure 5 pictures a part of the beam-pulser chassis. At left is the pulse generator (the copper casing is the primary) and at right is the vacuum tube switch.

REFERENCES

1. T. L. Khoo, et al., 1972-73 MSU Annual Report, p. 84(1973).

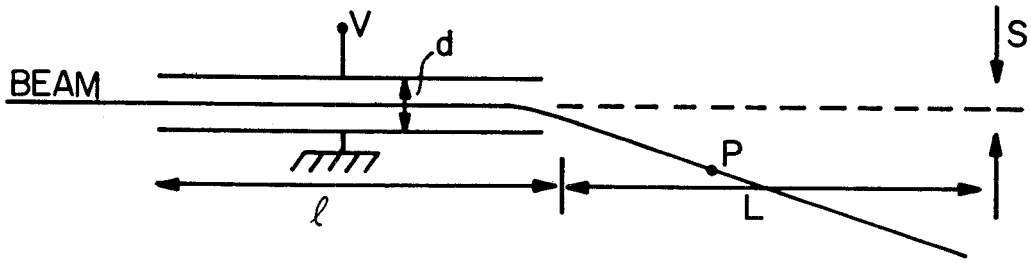

Fig. 1.--Positioning of the deflection plates in the beam line.

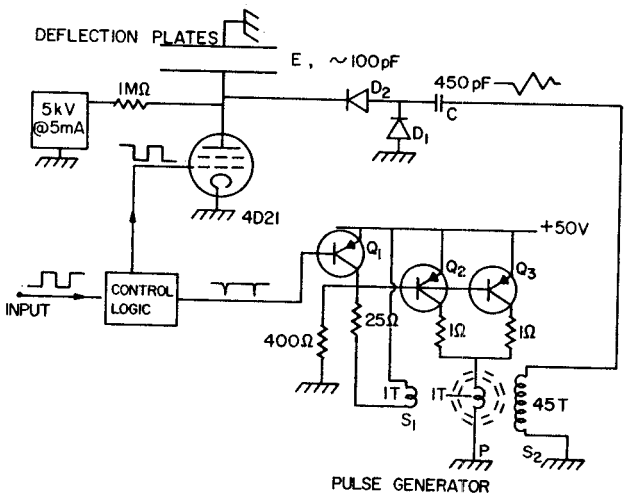

Fig. 2.--Symplified schematic diagram of the pulser.

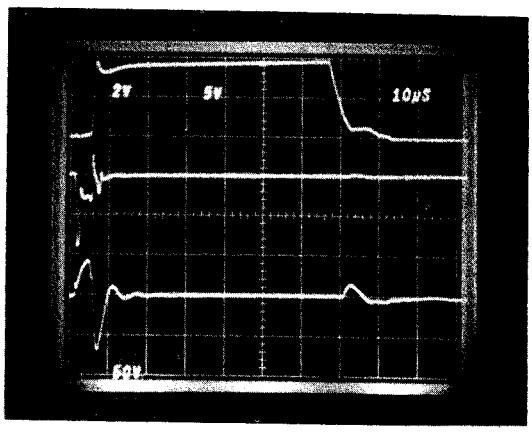

Fig. 3.--(u.t.) typical voltage on deflection plates. (2 kV/div)
(m.t.) primary current in the pulse transformer (10A/div).
(L.t) primary voltage in the pulse transformer (50V(div).

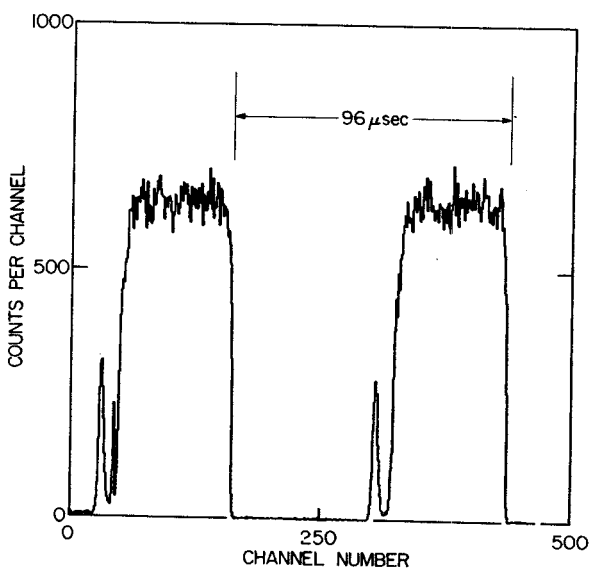

Fig. 4.--Typical beam intensity as function of time.

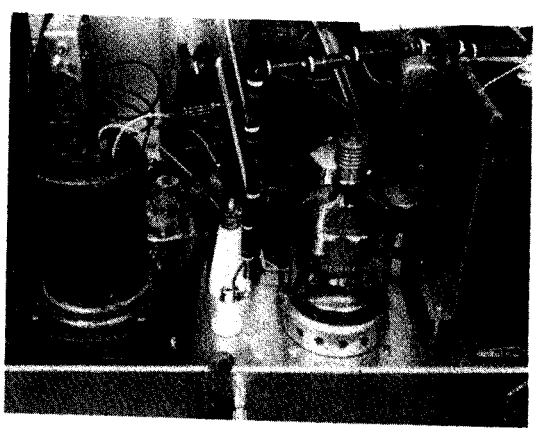

Fig. 5.--Close up view of pulse generator (left) and vacuum tube switch (right).

Position-Sensitive Proportional Counter Development

R. G. Markham and R.G.H. Robertson

The performance of charge-division, position-sensitive proportional counters is often very good (~0.3 mm resolution) for highly ionizing particles or particles incident normally, but becomes poor (~1 mm) in the common situation of low ionization and non-normal incidence. It has been known for some time that electronic noise is generally not the principal limiting factor.

At non-normal incidence the position signal represents the centroid of the ionization along the particle's trajectory projected onto the wire. It is our opinion that the chief factor leading to resolution degradation in that situation is statistical fluctuations in ionization along the path. In an early work, Miller et al.[1] attempted to calculate the effects of energy-loss fluctuations on position resolution. These calculations were based on the Bohr formula for the variance of the energy loss distribution. Unfortunately these calculations contained an error and grossly underestimated the severity of the problem.

Braid, Ford and Stoltzfus[2] have since performed a Monte-Carlo calculation with a Vavilov distribution of energy loss which is far more valid for particles with energies of interest. We also had independently calculated energy-loss fluctuation effects by direct integration of the distributions rather than by the Monte-Carlo method. Our results are shown in Fig. 1. For resolutions below about 1.6mm the curves should scale roughly as $\sqrt{D/P}$ where D is the depth of the counter and P is the gas pressure. Above ~1.6mm the curves flatten and become essentially pressure independent and scale as D. (The slight decrease at very high energies is probably artificial.) In all cases it was assumed that the intrinsic energy loss resolution of the counter was ideal. Other effects, such as statistical variations in multiplication, have not been considered yet, and will cause the curves of Fig. 1 to approach a lower limit.

Since the results of these calculations (and arguments) are in accord with our experience with these counters, we feel that these fluctuations are now the primary limitation. To avoid these problems one needs a device for which all the electrons along the ionization path will contribute to the computed position in the same manner. Thus, the position signal will be independent of energy-loss fluctuations along the path of the particle. A device for which this is approximately true is shown in Fig. 2. It differs from the usual type of counter in that a) the electron collection field is transverse to the particle trajectory (i.e., out of the paper) b) multiplication takes place on a plane of wires rather than a single wire, c) the position signal is induced on inclined pickup stripes close to the multiplication plane. Since the pickup stripes are parallel to the particle trajectories, this geometry gives position signals approximately independent of energy-loss fluctuations.

A prototype design showed that adequate signal strength was present on the pickup stripes. A circuit board containing the stripes connected by a thin resistive film has been constructed, by standard techniques,[3] to read out the stripes by charge division.

The present work is aimed at evaluating the resolution which can be achieved in this manner and also trying the very promising readout system of Iwata et al.[4] in which a commercial tapped delay line is connected to the sensing elements (pickup stripes in our case).

REFERENCES

1. G. L. Miller, N. Williams, A. Senator, R. Stensgaard, and J. Fischer, Nuc. Inst. Meth. 91, 389(1971).

2. J. Stoltzfus, private communication.

3. A. Ertel and J. R. Mars, Electronics, May 10, 1973, p. 109.

4. S. Iwata, E. Beardsworth, J. Fischer, M. J. LeVine and V. Radeka, B.A.P.S. 19, 528 (1974).

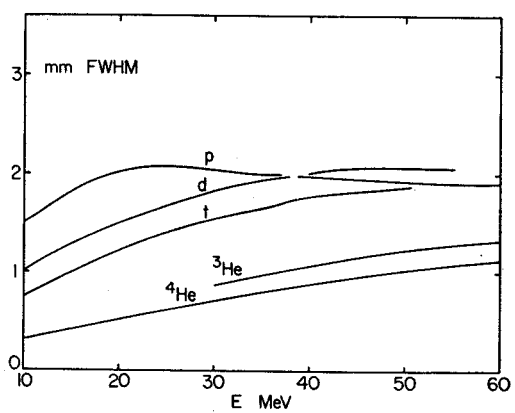

FIGURE 1.--The predicted contribution of energy loss fluctuations to the position resolution. The calculations were for 45° incident particles on a 1.5 cm thick counter filled with 95% (90% Ne+ 10% He) + 5% CO_2 at a pressure of one atmosphere.

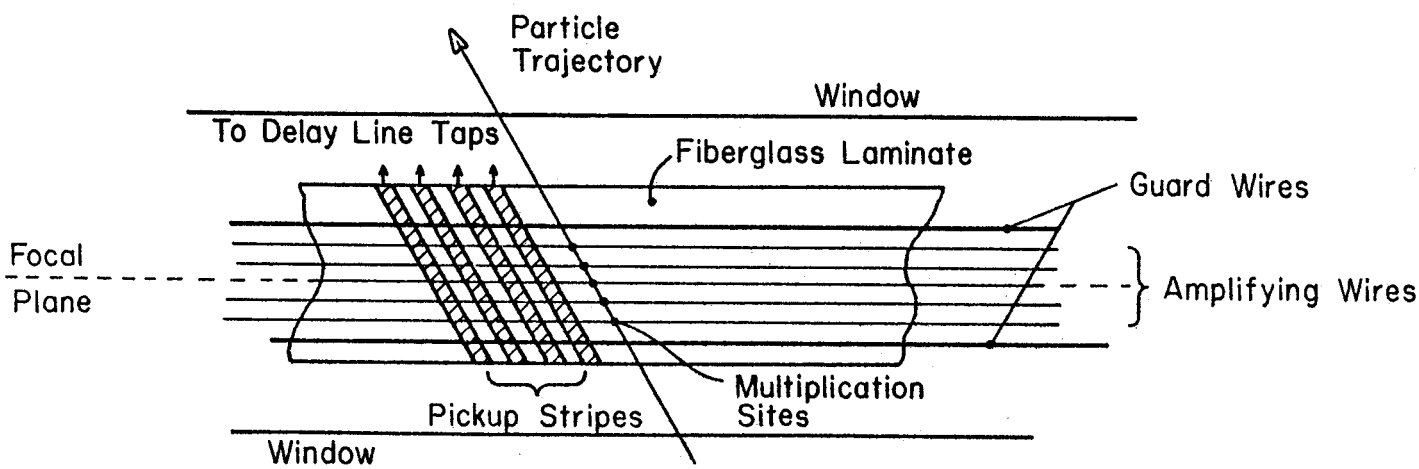

SCHEMATIC (Plan View) OF "WASHBOARD" COUNTER

Figure 2

A Counter Telescope with Two Dimensional Position Sensitivity

R. Markham, S. Austin and H. Laumer

A counter telescope having two-dimensional position sensitivity has been constructed. Its principle features are:

1. Large active area (400 mm^2)
2. Thin ΔE counter (as low as 300 $\mu g/cm^2$)
3. Time and energy resolution of a solid state device
4. Event location in two dimensions to better than 1.5 mm
5. Event rate capability in excess of 5 kHz.

The unit consists of a single-wire proportional counter directly followed by a solid-state detector (See Figure 1). The detector body is machined from a single block of aluminum with a separate front cover plate serving both as the front cathode and as window frame. The proportional counter wire--10 μm diameter nichrome--is mounted on wire extensions of a standard BNC vacuum feedthrough. Final tensioning of the wire is easily accomplished by slightly bending these extension wires. The solid state stopping detector is presently an Ortec 400 mm^2 fission detector which is held in place by its rear mounted Microdot connector mating with a Microdot vacuum feedthrough connector. Two types of entrance windows have been employed. The simplest to make is a gold coated mylar foil (~600 $\mu g/cm^2$). To achieve a thinner window, we have also used multiple layers of formvar supported by a mesh of 25 μm diameter tungsten wires. These windows have the following characteristics. The maximum transmission T_{MAX} of a wire mesh which will support a pressure P(atm) is given by: $T_{MAX} = 1 - 0.06\ P$. The minimum areal density ρ of formvar needed to hold pressure P on a wire mesh of transmission T is given by $\rho = 8P/(1-T)\ \mu g/cm^2$. The counter is generally operated with a gas filling of 90% Ar - 10% methane at one-tenth atmosphere. In this case for T=0.984 (T_{MAX}=0.994) and ρ=50 $\mu g/cm^2$ the total thickness of the ΔE counter is 320 $\mu g/cm^2$.

The horizontal position information (along the wire) is extracted using resistive charge division techniques. The fraction of the total charge induced on the wire that is collected at one end is linearly related to the position along the wire when low impedance preamplifiers are used. The vertical position information is extracted by directly measuring the time difference between the arrival of the signal from the stopping detector and the arrival of the signal from the proportional counter. The time delay of the proportional counter pulse--several hundred nanoseconds--is mostly due to the long transit time of the primary ionization electrons from the ionization track to the anode wire. Because the electric field falls off rapidly with vertical position and the electron drift velocity is a function of the field strength, the vertical response of the instrument is not linear, especially at large distances from the wire. (See Figure 2).

Numerous applications can be found for this device. The one which prompted its construction and for which it has been successfully used is the measurement (described elsewhere on this report) of the gamma width of the 7.66 MeV state of ^{12}C. The 7.66 MeV state was produced in the $^{12}C(\alpha,\alpha')^{12}C$ reaction and the telescope was used to identify recoiling ^{12}C nuclei in coincidence with scattered alpha particles. The position information was used to ensure proper alignment of the detectors and provide the optimum solid angle for detection of the recoils. Another promising use would be in channeling and blocking experiments where one would like to see a two dimensional distribution of events. The device also could be used as an ordinary counter telescope but with kinematic corrections being made via the θ-position information.

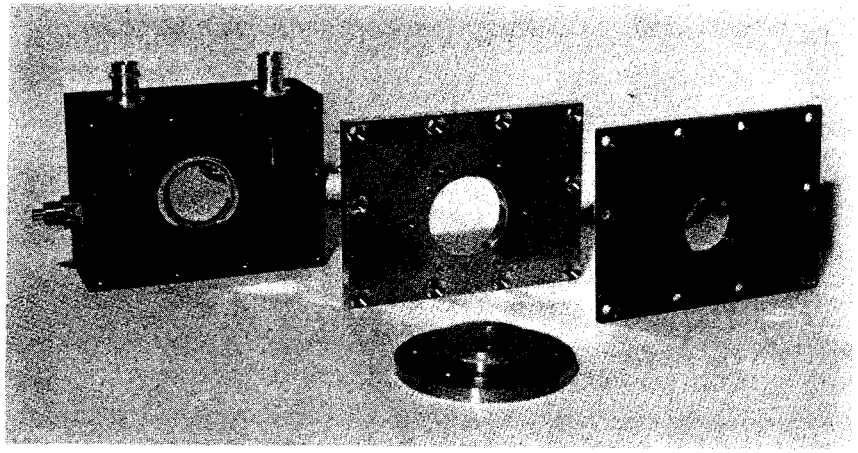

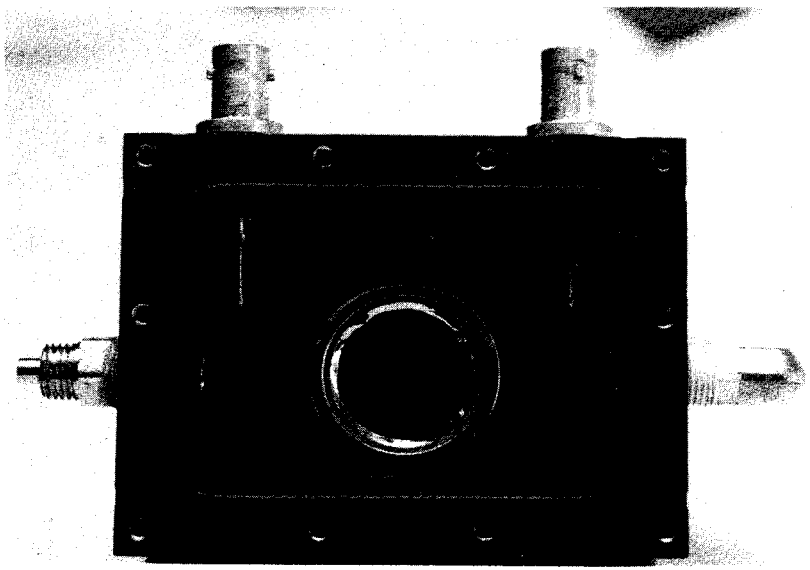

FIG. 1.--(a) The device is shown with two different front plates. The brass cover and detachable window frame are used with the wire-and-formvar windows. (b) A close-up view of the telescope. The proportional counter wire is mounted between the ends of the support wires.

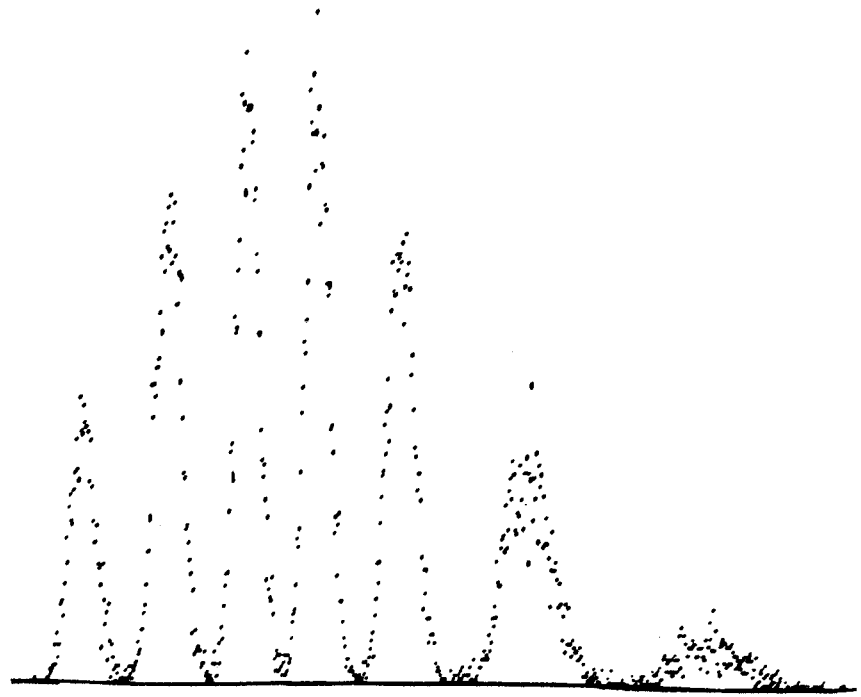

FIG. 2.--Shown is a vertical (drift time) spectrum of 10 MeV ^{12}C ions passing through a mask of horizontal slits. The slits are 0.8 mm wide and spaced 2.5 cm apart.

Progress on the MSU Time-of-Flight Spectrometer and Helium-Impurity Thermalizer-Transport*

M. D. Edmiston, K. L. Kosanke, Wm. C. McHarris, R. A. Warner, and W. H. Kelly

A time-of-flight mass spectrometer patterned after R. D. MacFarlane's MAGGIE system is nearing completion.[1] The spectrometer, in conjunction with MSU's helium-jet recoil transport system, will provide nearly on-line mass labeling of γ-ray and other spectra. We are aiming for mass resolution of one part in a thousand, which will be more than adequate since we desire to separate γ-ray energies coming from different isotopes.

The basic schematic of our apparatus was presented in last year's annual report.[2] That schematic is current except for a few minor changes. Since our prime interest is in γ-ray spectra rather than β information, we will derive timing signals from the Ge(Li) γ-ray detector rather than a β detector. This will require only a simple coincidence (start-stop) rather than a triple coincidence (start-stop-γ-ray event). In addition, the γ-ray signal will be delayed and used as the stop signal, using the positive ion detector (PID) as the start. This will eliminate much of the dead time since the timer will only start whenever a nucleus has interacted with the PID. A box flow-chart of the electronics is shown in Figure 1.

The PID is a channel-electron-multiplier-array (CEMA)--a ceramic disc containing many holes which are lined with low work-function material. Bias is applied across the disc and an ion impinging on a channel will start a cascade of electrons. Amplification is about 10^3; two will be used as a chevron detector to yield 10^6 amplification. The angles of the holes in the two arrays are dissimilar (yielding the chevron configuration) to prevent back-drifting ions from going further than half way, reducing the noise from backdrifting to 10^{-3} of the true signal. A cross section of the chevron detector is shown in Figure 2.

The precision digital delay we have chosen is a Berkeley Nucleonics Corp. Programmable Digital Delay Generator, Model 7030. It has a delay range of up to 99.999 μs in 1-nsec. increments. Its precision is about 0.01% of the delay and its stability is 1×10^{-5}/°C x delay.

Figures 3 and 4 show the progress on construction. All major parts are machined and assembled; vacuum plumbing and electrical wiring will be completed as this report is printed.

The rectangular box is pumped by a 16" vapor pump of the booster-ejector style and will operate around 10^{-3} torr. The helium jet will enter this box and the bulk of the helium will be removed by the skimmer. The cylindrical chamber contains the collecting surface, part of the flight path, and ports for Ge(Li) γ-ray detectors. This chamber is pumped by a 10" normal diffusion pump and will operate at about 10^{-6} torr. The initial flight path is 38 cm with a 68 cm piece being easily added.

Upon the completion of assembly we will begin initial tests to check resolution and efficiency while certain parameters are varied. Variable parameters include flight length, temperature and texture of the collecting surface, type of impurity in the helium-jet gas, etc. By early spring we hope to be ready to begin nuclear research. The prime area of interest will be γ-ray spectra of nuclei far from β stability. The apparatus should also be extremely valuable for the study of γ-ray spectra of fission fragments.

As an added feature, the construction has been contained on two platforms which are designed to be very portable. We can thus easily transport the apparatus to another laboratory to take advantage of unique equipment existing there. For example, we would like to take the machine to Los Alamos for some μ^--capture experiments.

*Supported by the U.S. Atomic Energy Commission and the National Science Foundation.

1. H. Jungelas, R. D. MacFarlane, and Y. Fares, Radiochem. Acta. 16, 141(1971).

2. MSU Cyclotron Annual Report 1972-73, p. 93.

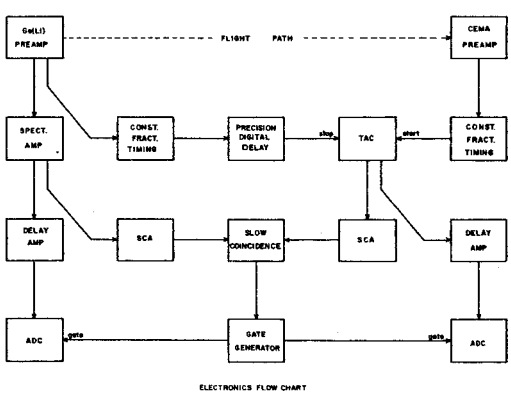

FIGURE 1.--Proposed logic for data handling.

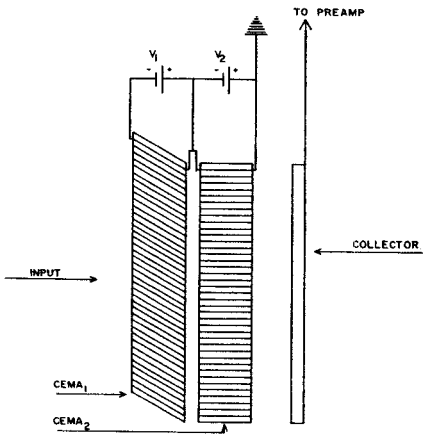

FIGURE 2.--Cross section of the chevron detector. The angle of the holes on $CEMA_1$ is 5° to the normal while $CEMA_2$ holes are 0°. $V_1+V_2 \leq 2800$ volts and $V_1:V_2$ is 3:5. The preamp input is held at +300V.

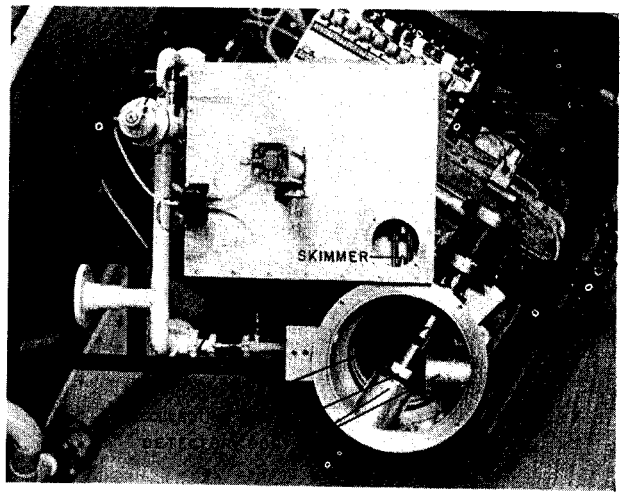

FIGURE 3.--View from top showing the two vacuum chambers. Rectangular chamber is 53.2 cm x 45.7 cm and round chamber is 38.1 cm O.D.

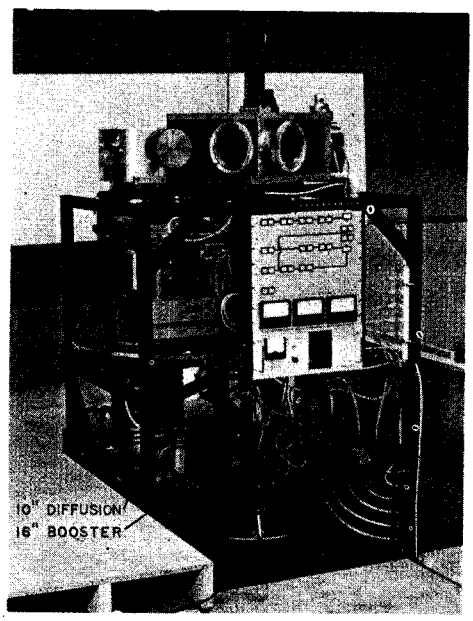

FIGURE 4.--View from side showing vapor pumps and supporting framework.

Helium-Jet Recoil Transport System*

K. L. Kosanke, M. D. Edmiston, Wm. C. McHarris, R. A. Warner and W. H. Kelly

Previous to this past year, our primary work involving our HeJRT system was a study of the system itself.[1] With the construction of a new laboratory and automated peripheral equipment for the HeJRT system[2] this past year has witnessed the transition to using our HeJRT system primarily as a research tool for the study of new nuclei. That part of our time still devoted to the study and development of the HeJRT system itself was directed toward its intended use as the first stage in our recoil time of flight system under construction (see page 86).

The taking of three types of nuclear data necessary to developing decay schemes have been simplified with the addition of peripheral equipment to the basic HeJRT system. The first is the collection of excitation functions in the search and identification of new nuclei. This was simplified with the addition of a remotely controlled absorber package ("Absorderdorber") to the modular constructed target assembly, see Fig. 1. This consists simply of a pair of motor-driver aluminum slides machined in places to various degrader thicknesses. One ranges from 0.000 to 0.056 cm (0 to 22 mil) is approximately 0.0076 cm (3 mil) steps, and the other from 0.00 to 0.51 cm (0 to 200 mil) is 0.064 cm (25 mil) steps. It is thus possible to degrade beams of light ions in sub-MeV steps. The slide positions are read out digitally to indicate degrader thickness. The second is the measurement of half-lives. After a half-life has been estimated from spectra collected at various tape speeds (tape transport is discussed elsewhere[1,2]) an accurate determination can be made using an automated system. A source is made while collecting on the tape while it is stationary. This source is then advanced to a detector where it is counted for timed intervals and stored as separate spectra. The source that was collected while counting was taking place is disposed of by advancing it past the detector. The procedure is then repeated. A 16-channel preset sequencer has been programmed to control all tape functions, to route the timed spectra in the computer and to turn on the cyclotron during the time a source is to be generated. In cases where the tape speed might be too slow, we anticipate using the sequencer to control a shutter assembly to interrupt the flow of activity from the capillary. The third is the collection of coincidence data. The arrangement of equipment for collecting Ge(Ci) - Ge(Ci) γ-γ multiparameter coincidence data is shown in Fig. 2. The detectors are slid into "top-hats" from opposite sides of the detector chamber for end-to-end geometry. (One detector can be slid in from an end of the chamber if 90° geometry is preferred.) There is a tapered, graded (Pb-Cd-Cu-Al) absorber between the detectors. The tape for these experiments is 1.27 cm magnetic computer tape and is run around the edge of the absorber. This geometry is very effective both in terms of detector solid angle and for eliminating Compton scattering between the detectors. (The geometry is not quite 180° because the activity on the moving tape is offset from the center line of the detectors.)

We have also had important success in the area of target fabrication for the HeJRT system. The most generally applied method involves pressing powdered target materials onto a foil (usually Al) backing. We use pressures in the range of 28,000 kg/cm^2 (200 ton/in.^{2}) generated with a hydraulic press [a 15,500 kg (17 ton) press purchased from an automotive parts supplier as a wheel puller]. Targets are now fabricated with the die set shown in Fig. 3; however, until recently a much less elegant apparatus was used with comparable results. Targets are normally 0.71 cm in diameter on a 0.005 cm (2 mil) Al backing previously affixed to a 2.5 cm circular frame. We typically use between 5 and 10 mg of target material, although targets using less material are possible with this procedure. This represents something of the order of a threefold savings over the amount of target material needed to reduce and evaporate a 1 mg/cm^2 target that might typically be used in a HeJRT system. Targets made with this pressing technique are extremely durable, oxide targets generally have a glassy appearance, an attempt to separate the target from the backing will generally destroy the backing before it can be accomplished. A final attractive feature of these targets is the small amount of time required to make one, normally less than 5 min. Some of the targets made recently with this technique for nuclear spectroscopic studies are oxides of ^{106}Cd, ^{141}Pr, and ^{144}Sm.

A second technique is just a modification of the technique where glue bonds a thin layer of target material to a foil backing. We have had surprising success with using a slurry of metal powders as target material and "Zip-Grip 10" (a moisture catalyzed poly-amide adhesive manufactured by Devcon Corp., Danvers, Mass.). (We have not investigated many other adhesives, but there are undoubtedly others that should work as well.) In our initial attempts we ground off the surface of the metal-Zip Grip composite in order to expose a surface of metal granules. However, we found this to be unnecessary and

found that no additional preparation is necessary. Targets that were untouched after the adhesive had setup gave recoil yields comparable to those that were ground. This was more than a little surprising, but presumably the coating of adhesive over the metal granules is thin enough not to interfere significantly with the recoils leaving the target. Again, as with the previous technique, the targets are durable, relatively inexpensive, and both quick and easy to make; however, this technique will not work with oxides that catalize the setting reaction of the adhesive, and, when attempted with these oxides, produces targets that lumpy globs of material. One target made recently with this technique is ^{92}Mo.

Fig. 1.--Exploded view of the target assembly. The parts from left to right are the vacuum window, absorderdorber, target holder, capillary exit, He supply, insulator, and water-colled Faraday cup.

Fig. 2.--View inside evacuated counting chamber set up for a γ-γ coincidence experiment. Activity is sprayed on the tape from the nozzle in the center, and circles the anti-Compton shield (not visible) between the cylinders surrounding the Ge(Li) cryostats.

Fig. 3.--Target die set.

REFERENCES

1. K. L. Kosanke, Ph.D. Thesis, Michigan State University, 1973.

2. K. L. Kosanke, M. D. Edmiston, R. A. Warner, R. B. Firestone, William C. McHarris, W. H. Kelly, submitted for publication in Nucl. Inst. and Methods.

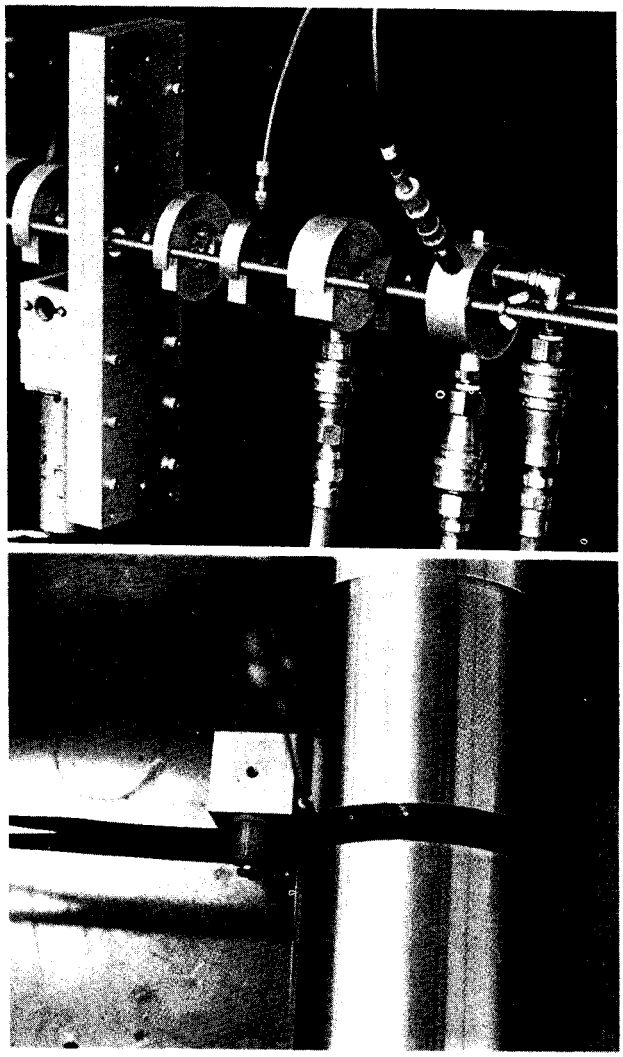

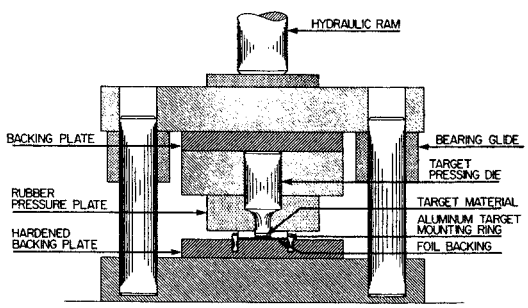

Target Making Laboratory

J. Nolen, H. Raut and D. Tody

During the past year approximately 250 targets were made in our laboratory. Many of these targets, prepared by techniques described in the 1972-73 Progress Report, will not be listed here. The new targets with condensed recipes are listed in the table. The majority of the targets are still made by evaporation from tantalum or tungsten filaments while a few are made via electron bombardment evaporation.

The ^{34}S target was made via a technique developed as an undergraduate research project. Layers of Formvar, carbon, and Formvar were laid down onto the target frame. Sulfur^{34} was evaporated with the gate valve closed from a tantalum tube filament onto the Formvar at ~2 x 10^{-4} torr. Another layer of Formvar was laid down, and sulfur was evaporated onto it. Only 1 mg of ^{34}S was used per evaporation. The final two layers were Formvar and carbon. All Formvar and carbon layers were ~2 $\mu g/cm^2$ and 20 $\mu g/cm^2$ in thickness, respectively. The sulfur layers were non-uniform, but this presented no serious problems in the experiments using this target. The combined thickness of the sulfur layers was approximately 180 $\mu g/cm^2$, and the carbon layers helped to prevent loss of sulfur due to vaporization in the beam. This is a variation of a technique described to us by Schiffer and Crozier of Argonne National Lab. (Mark Hedeman).

For the special purpose of studying the $^{14}C(p,n)$ reaction to the low-lying, widely-separated states of ^{14}N, a rather thick, epoxy-bonded target was made. On an area of 1 cm^2 2.5 mg of ^{14}C powder was mixed with 10 mg of a high-temperature epoxy which contained only C, H, and O. At 12.5 mg/cm^2 the target is still thin enough for the experiment at hand. Also, because the Q values for $^{12}C(p,n)$ and $^{16}O(p,n)$ are around -18 MeV and -17 MeV, respectively, compared with -0.6 MeV for $^{14}C(p,n)$, the large quantities of C and O are quite tolerable. ^{13}C, which can give neutrons in our region of interest, has an abundance in the target 1/30 that of ^{14}C. The activity of the target is 10 m Ci. The ^{14}C powder was handled with great caution before it was embedded in epoxy. (Michael Cabot, undergraduate research project).

Many of the oxides of separated isotopes have been reduced and evaporated sequentially in one continuous process through the use of high melting point reducing agents such as Zr, Ta, Th, or graphite powder. Zirconium powder has been very useful in reducing CaO because it does so at a much lower temperature than Ta powder and does not seem to contaminate the target. On the other hand, Zr reduction to MgO does lead to Zr impurity in the target so that Ta reduction at the higher temperature seems necessary in this case.

Attempts to reduce SrO_2 with Al, Zr, Ta, and Th powder proved unreliable due to the violent nature of the exothermic reaction. A satisfactory solution is to heat the SrO_2 in a Ta tube (crimped as in footnote 3 of the table) with no additional reducing agent added. The inside surface of the table is sufficient to reduce ~30 mg of the isotope in a nonviolent manner. Targets up to ~400 $\mu g/cm^2$ on thin carbon backings have been made via this method.

Studies are continuing in the use of a small, inexpensive glow discharge ion source for target making via sputtering. The goal is to make targets in the 100 $\mu g/cm^2$-2 mg/cm^2 thickness range of separated isotopes of such elements as Cr, W, Hf, and U. Initial tests have been promising in that 2 mg/cm^2 self-supporting W targets have been made by sputtering from W sheet. Currently improvements in the glow discharge gun are in progress and attempts to sputter from small quantities of powder will begin in the near future. This work is also an undergraduate research project (Ted Dyson).

A project to allow real-time target thickness measurements to be made during evaporation is currently in progress. The idea is to actually weigh the target during evaporation with a vacuum microbalance. This has two distinct advantages over the more conventional quartz crystal thickness monitor: Firstly, variations in sticking probability affect the accuracy of the quartz crystal method because the target of interest is evaporated onto a different substrate while merely being monitored by the nearby crystal. Secondly, much higher efficiency will be attainable by the close working distances feasible with the direct microbalance method. The crystal requires larger working distances so that the distribution of evaporation material will reach both the crystal and the separate target substrate. Recent tests of the vacuum microbalance indicate a probable accuracy of ~10 $\mu g/cm^2$ in an actual evaporation. Apparatus modifications to adequately shield the microbalance and to make it relatively convenient to use are currently in progress.

Other current projects include modifications and expansion of target storage facilities. There are ~100 targets currently stored in the atmosphere, ~100 stored in roughing pump vacuum (which are transferred in air when used), and ~10 targets stored in a high vacuum with a vacuum lock transfer system. The high vacuum storage facility has been redesigned and construction is

now nearly complete. Vacuum testing is currently in progress. The new system has storage capacity for 90 targets, an improved vacuum lock transfer mechanism, and fail-safe vacuum logic.

TABLE.

Target Element	Chemical form of target	Starting Material	Method of Fabrication	Backing[1]	Thickness ($\mu g/cm^2$)	Amount of Isotope required for 100 $\frac{\mu g}{cm^2}$ (mg)	Remarks
Li	Li	Li	Vac. Evap. Ta, W dimple boat	S.S.	>300		By scraping from glass substrate
$^{10,11}B$	B	B	Electron Bomb.	S.S. Formvar	100-300 ~600	10	S.S. & Formvar by Sucrose + Betaine Floatation[6]
				C	≤300		Multilayer sandwich w/ Formvar
C	C	C	Decomposition of CH_3I	S.S.	>500		Separation from Ta substrate
N	Adenine	Adenine	Vac. Evap, Ta point source[3]	C	≤200		
	Melamine	Melamine	Vac. Evap, Ta point source	C	≤10,000		
^{29}Si	Si+SiO	SiO_2	Vac. Evap,[5] Ta point source,w/Ta powder	S.S. Formvar C	~300 <250	3	S.S. & Formvar by CSI floatation
^{34}S	S	S	Vac. Evap., Ta point source	C	~200	1	Evap. 1 cm. distance Multilayer sandwich w/c+ Formvar.
K	K	KCO_3	Vac. Evap,[5] Ta point source	C	<200		
	K Cl	K Cl	Vac. Evap, Ta point source	C	<200		
$^{40,42,44}Ca$	Ca	$CaCO_3$	Vac. Evap,[5] Zr point source,[3] w/Zr powder	S.S.	>500	5	By scraping from glass substrate
^{50}Cr	Cr	Cr_2O_3	Electron. Bomb,[5] C,Crucible,w/c powder Vac. Evap,[4] Ta point source, w/ta powder	C	<100	5	
				C	<200	5	
^{61}Ni	Ni	Ni	Vac. Evap, W-dimple boat	C	<250	3	
^{63}Cu	Cu	CuO	Vac.Evap,[5] Ta point source,w/Ta powder	S.S.	>100	2	By CSI flotation
$^{116,120,124}Sn$	Sn	SnO_2	Vac.Evap,[5] Ta point source,w/Ta powder	S.S.	300-1500	2	By CSI floatation
^{140}Ce	CeO_2	CeO_2	Electron. Bomb, Ta crucible vac. evap., C. Boat Ta point source	Formvar C(5 $\mu g/cm^2$)	~200 ≤100	30	Evap. 10cm. distance sucrose +Betaine floatation for formvar
$^{161,163}Dy$	Dy	Dy_2O_3	Vac. Evap,[4] Ta point source, w/Th powder	C	<200	10	
Er	Er	Er_2O_3	Vac. Evap,[4] Ta point source, w/Th Powder	S.S.	>500		Deposit on Ta. Ta dissolved in 1:1,HF,HNO_3
$^{184,186}W$	WO_3	WO_3	Vac. Evap.,Ta point source	Formvar C Al	~500 <400 ~400		CSI floatation for formvar.
U	U	U	Vac. Evap., W dimple boat	C	≤50		

TABLE.--Continued.

*Impurity from filament likely.

[1]S.S. means self supporting targets and C usually means 20 $\mu g/cm^2$ Carbon plus formvar.

[2]Amount for evaporation at approximately 3 cms. distance in most cases.

[3]Ta or Zr point source means tube with ends smashed and small hole drilled on its side.

[4]Reduction is carried out and the isotope is condensed inside Ta tube boat, turned upside down. Then evaporation is done from Ta tube boat.

[5]Simultaneous reduction and evaporation.

[6]Betaine-Monohydrate and D^+ Sacharose (mixing ratio: 7:1) dissolved in distilled H_2O.
P. Maier-Komor, Proceedings of Third International Symposium on Research Materials[2]for Nuclear Measurements, Oak Ridge National Lab (1971).

Automatic Plate Scanner

J. Nolen and R.G.H. Robertson

Several tests, improvements, and modifications of the automatic plate scanner have been made during the past year. The pre-amp and track discrimination circuitry has been improved to yield extremely good signal to noise ratios on relatively dim high energy proton tracks, as well as the brighter tracks such as deuterons and tritons.

The photographs show typical tracks signals and illustrate the basic logic operations in track discrimination. To be counted a signal must rise above a DC level for less than a preset time interval and the rise time must also be less than a preset value. The present logic, however, does not insure proper track count normalization because a single photodiode slit equal to one track length is being used. Since the stage step size is also one track length, a given track may be counted twice or not at all if it overlaps the diode about one-half on each of two successive steps. An extension from the present "relative" single diode logic to an "absolute" three diode system is currently planned.

The current "relative" scanning mode is already quite useful, however, and it will be used as soon as some mechanical modifications of the stage are completed. One of these modifications which is completed but not fully tested is an improved plate holder. This plate holder, designed to overcome a rather serious focussing problem, is quite rigid and flat. The glass plates are flattened somewhat by forcing them against the two parallel edges of this holder in an attempt to keep the surface of the emulsion in focus at all times as the plate is moved by the stage under the microscope. Another modification currently in progress is a permanent mount with focussing and positioning controls for the new 35 watt Xe arc lamp illumination source. This light source has been fully tested and works well otherwise.

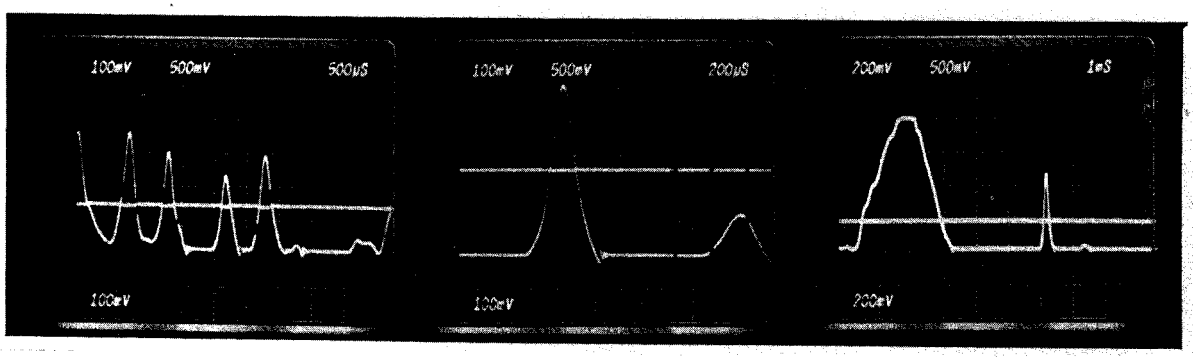

(a) Electronic signals from the photodiode for 30 MeV proton tracks.

(b) Signals from 25 MeV deuterons in the same emulsion (NTB 25 μm) as (a).

(c) Trace at 1/2 sweep speed of (a) to show "dirt" is typically wider and has slower rise time than "track".